A Zinc Oxide-Perylene Diimide Hybrid Electron Transport Layer for Air-Processed Inverted Organic Photovoltaic Devices

*Edward Cieplechowicz,[a] Rahim Munir,[a] Michael A. Anderson[b], Erin L. Ratcliff[b,c,d], Gregory C. Welch[a]**

[a]Department of Chemistry, University of Calgary, 2500 University Drive N.W., Calgary, Alberta, T2N 1N4, Canada
[b]Department of Materials Science and Engineering, University of Arizona, Tucson, AZ 85721, USA.
[c]Department of Chemical and Environmental Engineering, University of Arizona, Tucson, AZ 85721, USA.
[d]Department of Chemistry and Biochemistry, University of Arizona, Tucson, AZ 85721, USA.

Email: gregory.welch@ucalgary.ca

Keywords: Organic Photovoltaics, Cathodic Interlayer, Perylene Diimide, Slot-Die Coating, Green Solution Processing

Abstract: In this work, we report the formation of perylene diimide films, from green solvents, for use as electron transporting layers, when combined with ZnO, in inverted type organic photovoltaics. A modified N-annulated PDI was functionalized with a *tert*-butyloxycarbonyl protecting group to solubilize the material enabling solution processing from green solvents. Post deposition treatment of films *via* thermal annealing cleaves the protecting group yielding the known PDIN-H material rendering films solvent resistant. The PDIN-H films were characterized by optical absorption spectroscopy, contact angle measurements, and atomic force microscopy. When used to modify the surface of ZnO in inverted type organic photovoltaics (air processed and tested) based on the PM6:Y6 and PTQ10:Y6 bulk-heterojunctions, the device power conversion efficiency increases from 9.8% to 11.0% and 7.2% to 9.8%, respectively.

1.0 Introduction

Semiconducting films comprised of π-conjugated organic molecules or polymers are effective as electron transporting materials in organic photovoltaic (OPV) devices for the conversion of solar energy to electricity.[1,2] Inverted type OPV devices exhibit high environmental stability because silver can be used as a top electrode. These devices typically use zinc oxide (ZnO) films as an electron transport layer (ETL) atop indium tin oxide (ITO) bottom electrodes.[3,4,5] ZnO is commonly used owing to a high electron mobility, facile solution processing into uniform films, optical transparency in the visible region, and a low work function appropriate for electron extraction.[6,7] However, there are several drawbacks to ZnO such as non-ideal ohmic contact with organic photoactive layers that can lead to electron traps and increased resistances/recombination within devices, as well as sensitivity to moisture of the pre-deposition solutions leading to poor device reproduciability.[8,9] In addition, OPV devices using ZnO ETLs require "light soaking" to achieve optimal performance.[10,11] To circumvent most of these issues, the ZnO ETL can be modified with interfacial materials (between the photoactive layer and ZnO) to enhance performance and stability. A wide variety of materials have been designed to modify ZnO and enhance OPV performance.[2,12]

Modification of ZnO with various interfacial materials has been investigated using both conjugated small molecules and polymers. This has been achieved using self-assembled monolayers (SAMs)[13,14] and distinct film formation atop the ZnO layer.[2] These interfacial materials are crucial in mitigating physical defects on the ZnO surface that can lead to charge traps and carrier recombination,[15] as well as chemical defects such as surface hydroxide (-OH) which can generate radicals upon excitation.[14,15] Perylene diimides (PDIs) have proved effective for interface engineering due to facile functionalization allowing for selective attachment and

appropriate electron affinity allowing for energy level alignment between ZnO and fullerene/non-fullerene acceptors within the photoactive layer.[16,17]

Tailor-made PDIs for use as ETLs in OPVs have proven to be quite effective at boosting device performance by facilitating electron injection into the cathode.[17–20] Yu *et al*. reported an amine functionalized PDI (PDIN) at the imide positions (Figure 1a), which is processed from methanol into ETL films atop of ZnO, and improved charge transport, boosting the power conversion efficiency (PCE) of PTB7-Th:B-DIPDI based devices from 5.52% to 6.29%.[18] Li *et al.* modified PDI with methyl phenol groups via ether linkages and bare imide positions giving PDI-H (Figure 1b).[19] PDI-H was processed from a mixture of methanol and tetrahydrofuran atop ZnO and thermally annealed to improve the PCE of both P3HT:$PC_{61}BM$ and PTB7-Th:$PC_{71}BM$ based devices from 3.51 % to 4.78 %, and 8.33 % to 10.31 %, repesctively.[19] Wen *et al.* reported a tetrahydroxy functionalized PDI at all four bay positions to yield the twisted material PDI-OH (Figure 1c).[20] PDI-OH was co-processed with ZnO to give a hybrid ETL to improve the PCE of PBDB-T-2Cl:IT4F based devices from 12.28 % to 13.30 %. In addition a top PCE of 15.95 % was achieved for PBDB-T-2F:Y6 based devices.[20] Abd-Ellah *et al.* modified an N-annulated PDI with a pendant carboxylic acid (PDIN-Acid, Figure 1d), which was processed atop ZnO to improve the performance for various OPV devices based on PPDT2FBT:$PC_{61}BM$ (5.2 % to 6.3%), PPDT2FBT:ITIC-M (6.9% to 7.2%), and PPDT2FBT:PDI_2N-EH (5.8% to 6.4%) active layers.[17]

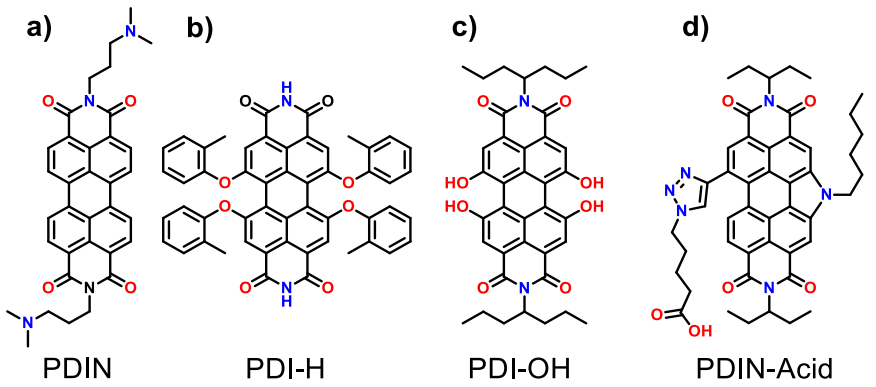

Figure 1: Chemical structures of PDI compounds used as electron transport layers in combination with ZnO for OPV devices. A) PDINO,[18] B) PDI-H,[19] C) HO-PDI,[20] and D) PDI-Acid[17].

Recently, Harding *et al*. demonstrated that the deprotonation of the insoluble compound PDIN-H lead to the formation of an ion pair (PDIN-Na) with alcohol solubility. Upon film formation (*via* spin-coating or slot-die coating), the PDIN-Na material spontaneous protonates, analogous to the acid dyeing process, to yield PDIN-H, which proved an effective ETL (in combination with ZnO) for inverted type OPV devices (Figure 2a).[16,21] The ZnO/PDIN-H hybrid ETL is attractive for OPV scale-up owing to the increased device stability and facile processing via slot-die coating. Limitations include the caustic hydroxide base required and limited solvent processing window (i.e., alcohol only).

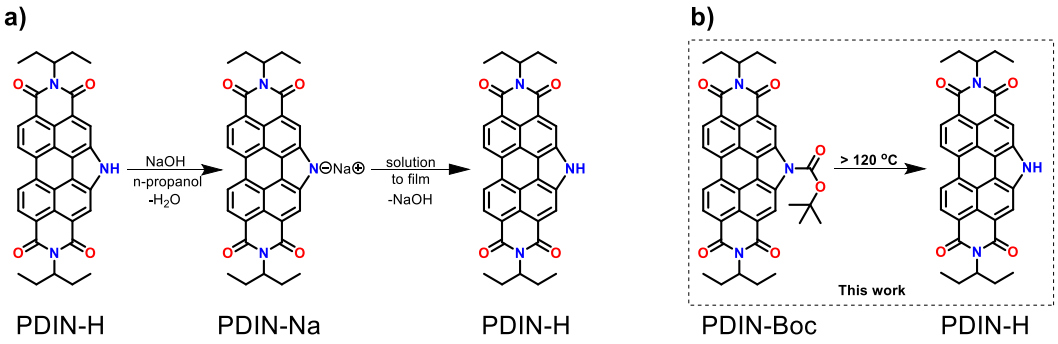

Figure 2: a) Chemical structures of PDIN-H and PDIN-Na. The PDIN-Na ion pair is soluble in alcohols and upon film formation, spontaneous protonation occurs, yielding PDIN-H films, which are solvent resistant.[21] b) Chemical structure of PDIN-Boc and conversion to PDIN-H. The strategy presented in this work centers on the thermal deprotection of PDI-Boc to yield PDIN-H films for use an electron transport layers, in combination with ZnO, in OPV devices.

To expand the scope of processing, we introduce an N-annulated PDI functionalized with a *tert*-butyloxycarbonyl (Boc) protecting group (Figure 2a). Here the Boc protecting group renders the PDI compounds soluble in a range of polar and non-polar organic solvents, consistent with lierature,[22–24] allowing for increased processing options, and can be thermally removed in the film to yield the desired PDIN-H. The Boc protection/deprotection strategy has been used effectively with indigo, isoindigo, and diketopyrrolopyrrole dyes for applications in field-effect transistors,[22,23] and OPVs.[24] Herein, we report on the synthesis of PDIN-Boc (Figure 2b), film formation from the green organic solvent 2-methyl anisole *via* both spin and slot-die coating, thermal deprotection to form films of PDIN-H (Figure 2b), and utility as an ETL in combination with ZnO for air-processed OPV devices.

2.0 Results

2.1 PDIN-Boc Synthesis and Characterization

The compound PDIN-Boc (**5**) was synthesized from the commercially available perylene tetracarboxylic dianhydride (**1**) (Scheme 1, experimental details in the Supporting Information). Compound **2** and **3** were synthesized as previously reported.[25] Compound **4** was synthesized using a modified literature procedure where dimethylformamide (DMF) solvent was replaced with *o*-xylene, enabling to higher reaction temperature to be used without formation of side products, thus simplifying product purification and leading to near quantitative product formation. PDIN-Boc (**5**) was prepared using a modified literature procedure.[26]

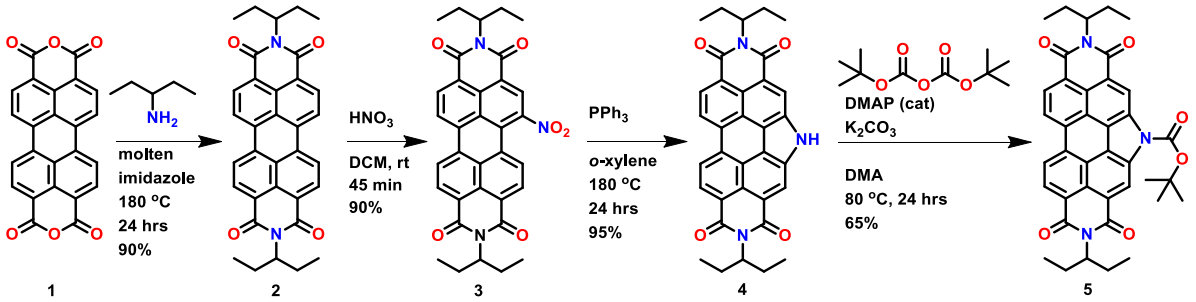

Scheme 1: Synthesis of PDIN-Boc (**5**) from commercially available starting materials. Full details are found in the Supporting Information. DCM = dichloromethane, DMA = Dimethylacetamide, DMAP = 4-Dimethylaminopyridine.

PDIN-Boc (**5**) was characterized by ^{1}H and ^{13}C NMR spectroscopy, mass spectrometry, cyclic voltammetry (CV), differential pulse voltammetry (DPV), thermogravimetric analysis (TGA), and infrared spectroscopy (IR) (see Supporting Information). Thin films of both PDIN-Boc and PDIN-H were characterized using ultraviolet-visible spectroscopy (UV-vis), contact angle measurements, and atomic force microscopy (AFM) (*vide infra*). PDIN-Boc was found to be soluble in a range of halogen-free solvents, including the food additive 2-methyl anisole (Figure S11), making PDIN-Boc compatible with OPV module fabrication.[27–29] For this work, we focused on film processing from 2-methyl anisole due to its elevated boiling point allowing for control deposition and the simple fact that the solvent is non-toxic to humans and the environment.[27]

2.2 – PDIN-Boc Thermal Conversion to PDIN-H

The thermal *in-situ* deprotection of PDIN-Boc was investigated using both TGA and thin-film UV-vis spectroscopy (Figure 3). TGA data was obtained at a rate of 1 °C/min and showed that the PDIN-Boc deprotection began at 100 °C and was complete one hour later at 160 °C, affording PDIN-H (Figure 3a). The PDIN-H thermal stability persists to 380 °C, at which point the imide sidechains began to degrade. The deprotection can also be tracked *via* UV-vis spectroscopy using thin films cast from 2-methyl anisole (Figure 3b). The spectrum of a PDIN-Boc film has a λ_{max} at 485 nm (Figure 3b). After heating at 200 °C for 20 minutes, λ_{max} is red-

shifted to 530 nm (Figure 3b), consistent with the formation of PDIN-H. The deprotection can also be observed visually with an orange to red color change (Figure 3-c).

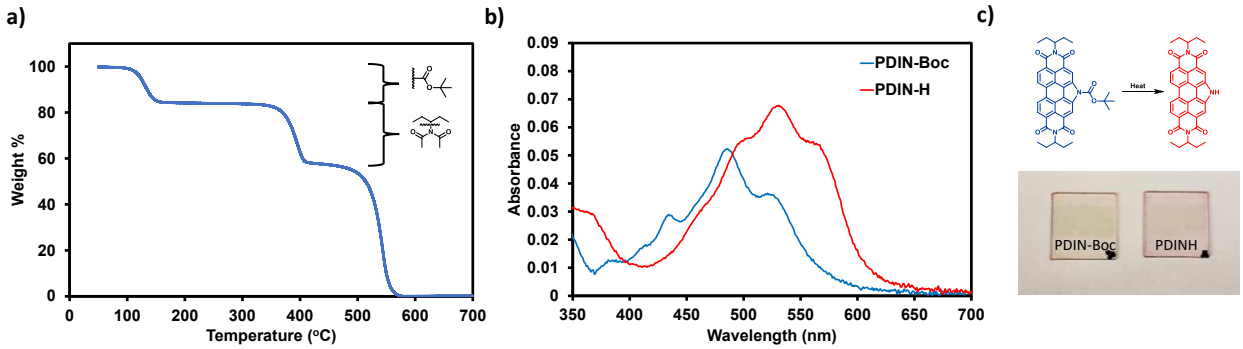

Figure 3: a) TGA plot of PDIN-Boc at a heating rate of 1 °C per minute. Thermal deprotection starts at 100 °C and is complete at 160 °C. b) Optical absorption spectra of PDIN-Boc thin film atop a glass/ITO/ZnO substrate (spin-cast from 10 mg/mL 2-methyl anisole solution) before annealing (blue) and the same film annealed at 200 °C for 20 minutes, converting to PDIN-H (red). c) PDIN-Boc thin films (spin-cast from 10 mg/mL 2-methyl anisole solution) on glass/ITO/ZnO substrate: (left) before annleaing (organe) and (right) after annealling (red). The PDIN-Boc film is thermally converted to the PDIN-H film.

The thermal deprotection was investigated at 120, 160, and 200 °C using films cast from PDIN-Boc solutions in 2-methyl anisole (1, 5, 10 mg/mL) to determine the efficacy of the thermal annealing process (Figure S12-14). Thin-films of PDIN-Boc could be converted to PDIN-H at 120°C in 40 minutes (for films cast from 1 mg/mL solutions) and 100 minutes (for films cast from 5 mg/mL solutions), while thicker films (cast from 10 mg/mL solutions) could be fully deprotected after 120 minutes. Heating all PDIN-Boc films at 160°C or 200°C resulted in complete deprotection within 40 and 20 minutes, respectively. Deprotection does result in changes of film crystallinity. Most notably the lamellar out-of-plane distance decreases which is consistent with the loss of the BOC group bringing molecules in vertical alignment closer together (Figures S23), as observed through GIWAXS measurements. Recognizing the importance of OPV scale-up and flexible OPV modules, the PDIN-Boc deprotection was evaluated on polyethene terephthalate (PET) substrates, where PDIN-Boc films were formed via slot-die coating and subjected to thermal

annealing at 120°C. Completed conversion to PDIN-H was observed with no deformation of the PET substrates (Figure S15).

2.3 – PDIN-Boc and PDIN-H Film Formation on ZnO

Surface wettability of a material is important for understanding the compatibility between layers within an OPV device. Coating organic materials atop high energy surfaces (metal oxides and ionic) is often problematic, as it can lead to poor organic film formation.[30] Passivation of metal oxide surfaces can be carried out to allow for improved photoactive layer film formation.[14] Modifying the high energy ZnO with a cathodic interlayer material lowers the overall surface energy of the ETL. This in turn promotes better contact between ETL and the organic materials of the BHJ, leading to improved charge transport.[14] Thus the surface energy of ZnO, ZnO/PDI-Boc, and ZnO/PDIN-H films were probed using water contact angle measurements (Figure 4).

Films of PDI-Boc were spin-cast atop glass/ITO/ZnO substrates (standard for inverted OPV devices) at three different concentrations (1 mg/mL, 5 mg/mL, and 10 mg/mL in 2-methyl anisole). For neat ZnO, water contact angles were measured to be 30° (Figure 4a). ZnO/PDIN-Boc films had an increased water contact angle upwards of 57° (Figure 4b). After thermal deprotection (200°C for 20 minutes) to give ZnO/PDIN-H films, the water contact angle further increased upwards of 70° (Figure 4C). The data is consistent with the elimination of the polar Boc protecting group and the formation of PDIN-H which is a hydrophobic film.

The surface of the films was further probed using AFM (Figure S16). ZnO films were relatively unfirm with an RMS of 1.68 nm. The ZnO/PDIN-Boc films were uniform with no significant changes in surface roughness. Upon thermal annealing and the formation of the ZnO/PDIN-H films a smoothening was observed with an RMS value as low as 1.08 nm. Together

these results confirm that the ZnO/PDIN-H films are smooth and hydrophobic and thus appropriate for deposition the organic photoactive layer on top.

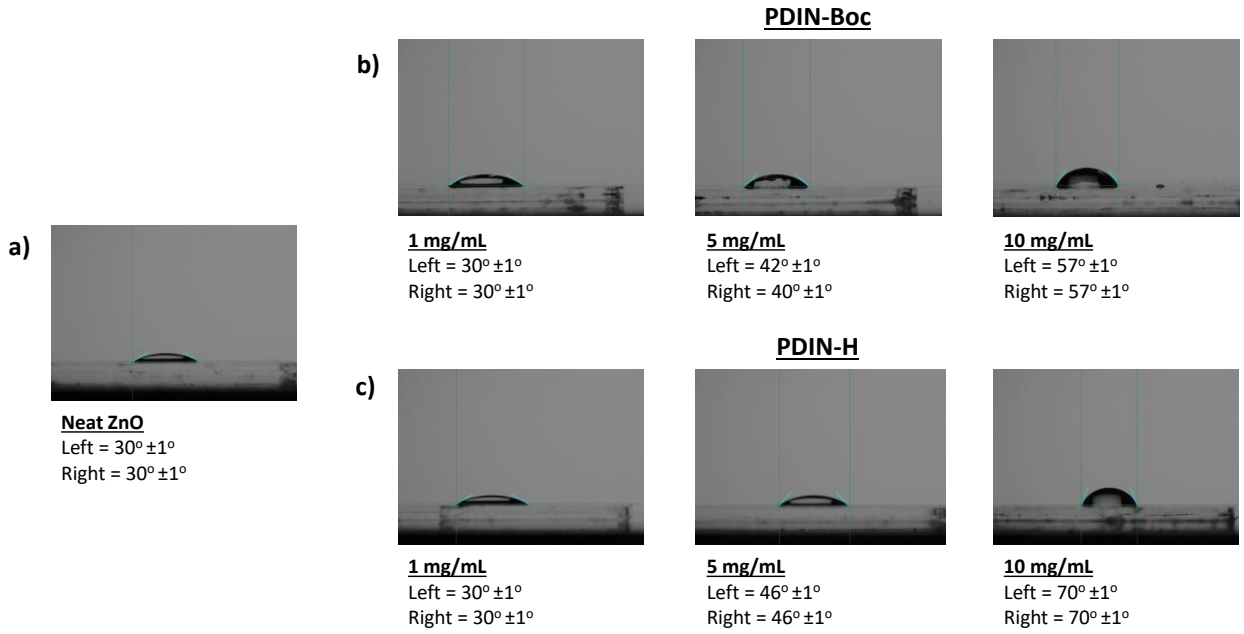

Figure 4: Water contact angle measurements: a) water on a glass/ZnO film, b) water on glass/ZnO/PDIN-Boc films (PDI-Boc films spin-cast from 1, 5 and 10 mg/mL 2-methyl anisole solutions), c) water on glass/ZnO/PDIN-H films (after thermally annealing at 200°C for 20 minutes).

Section 2.4 - PDIN-Boc and PDIN-H Film Solvent Resistance

For all solution processed OPV devices, the solvent compatibility between the functional layers is crucial to ensure distinct and uniform multi-layer device construction.[31] Considering that the photoactive layers would be solution deposited onto the PDIN-H layer, we investigated the solvent resistance (or insoluble nature) of the films. For this purpose, a selection of common photoactive layer processing solvents was spin-cast atop both the ZnO/PDIN-Boc and ZnO/PDIN-H films and analyzed by UV-vis spectroscopy (Figure 5). A decrease in absorbance can be attributed to degradation of the film by the wash solvent. The optical absorption spectra of

ZnO/PDIN-Boc films before and after casting the solvents *o*-xylene, 2-methyl THF, $CHCl_3$, toluene, *o*-dichlorobenzene, and 2-methyl anisole, show a large decrease in light absorption, indicating that the film was washed away (Figure 5-blue). In contrast, the optical absorption spectra of ZnO/PDIN-H films remain intact after solvent casting on top, with only a slight decrease in absorption when chlorinated solvents were used (Figure 5-red). Same trends were observed for thinner and thicker films (Figures S17 and S18).

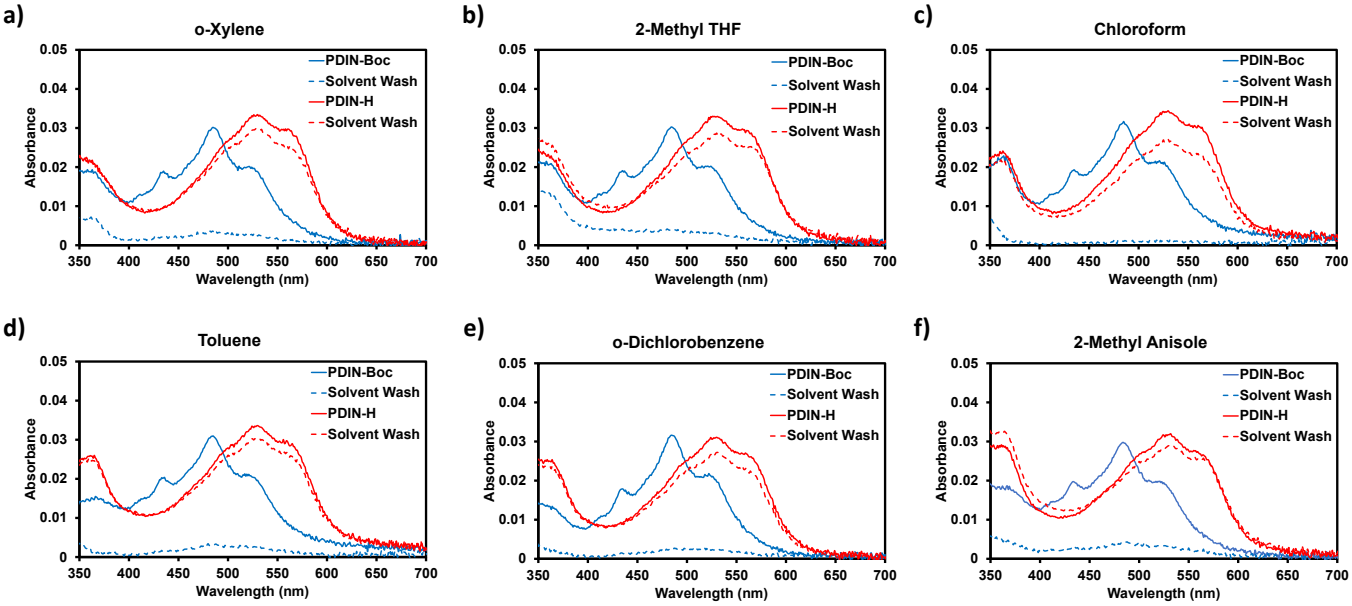

Figure 5: Solvent resistance of ZnO/PDIN-Boc and ZnO/PDIN-H films. Optical absorption spectra of glass/ZnO/PDIN-Boc (blue) and glass/ZnO/PDIN-H (red) before and after solvent washing: a) *o*-Xylene, b) 2-methyl THF, c) chloroform, d) toluene, e) *o*-dichlorobenzene, and f) 2-methyl anisole. The solvents (100 µL) were spin-cast on top of the films and allowed to dry prior to measurement. PDIN-Boc films were spin-cast (5 mg/mL in 2-methyl anisole) on top of glass/ZnO. PDIN-H films formed by thermally annealing the glass/ZnO/PDIN-Boc films at 200°C for 20 minutes.

Section 2.5 – PDIN-H Film Utility in Organic Photovoltaic Devices

Next the ZnO/PDIN-H hybrid film (where PDIN-H films were formed by converting PDIN-Boc films via thermal annealing) was used as a ETL in inverted OPV devices using photoactive layers comprised of Y6 and various donor polymers.[32] Donor and acceptor pairs of

PTQ10:Y6[33] and PM6:Y6[32] were chosen to fabricated the bulk-heterojunction (BHJ) photoactive layers and evaluate device performance. An inverted architecture was used for the OPV devices with structures: ITO/ZnO/BHJ/MoO_x/Ag and ITO/ZnO/PDIN-H/BHJ/MoO_x/Ag, directly comparing the impact of the PDIN-H layer. The energy levels of all components used in OPV device fabrication, as well as a schematic view of the device architecture, are shown in Figure 6.

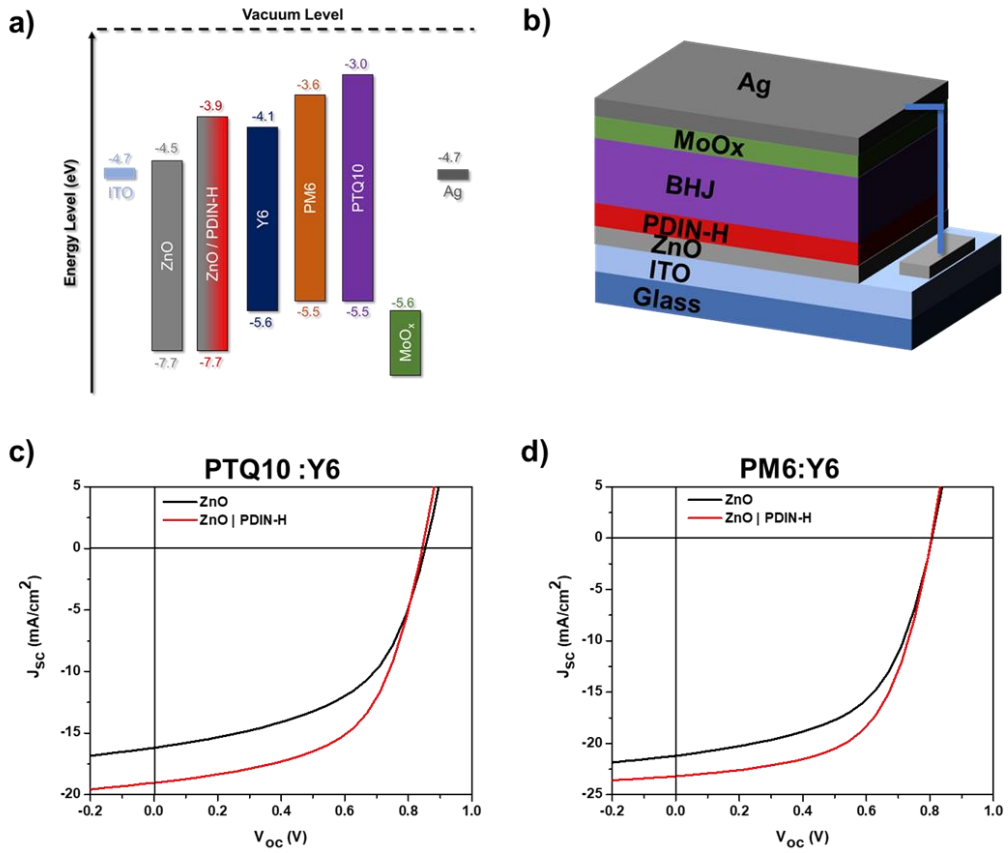

Figure 6: a) Energy level diagram of components used in the fabricated OPV devices: ITO,[16] ZnO,[16] ZnO/PDIN-H,[16] PM6,[34] PTQ10,[35] Y6,[32] MoO_x, and Ag. (note: either ZnO or ZnO / PDIN-H is used as the ETL). b) Schematic view of the device architecture. J-V curves of OPV devices based on c) PTQ10:Y6 BHJ spin casted at 2500 rpm and d) PM6:Y6 BHJ spin casted at 3000 rpm, with (red) and without (black) PDIN-H layer.

All the solution processing for the device fabrication and testing was conducted in an ambient environment. Chloroform was used as the deposition solvent for BHJ formation. The current voltage (J-V) curves of the OPV devices are shown in Figure 6(c,d), and the device

parameters are listed in Table S1. When PDIN-H is employed in an OPV device with PTQ10:Y6 blend, we observe an increase in device PCE from 7.2% to 9.2% when the BHJ was spin cast at 2500 rpm (Figure 6c). We also tested other BHJ spin coating speeds (2000 and 3000 rpm) and observed a similar increase in PCE (Table S1). The OPV devices with PM6:Y6 blend also show an increase in device PCE, with PDIN-H layer, from 9.8% to 11.0% when the BHJ is spin cast at 3000 rpm (Figure 6d). Again, we tested more BHJ spin coating speeds (2000 and 2500 rpm) and observed a similar increase in device PCE (Table S1). The J-V curves of individual devices are shown in supporting information (Figure S20). The statistical data of V_{oc}, J_{sc}, FF, and PCE with respect to BHJ spin coating speed, with and without PDIN-H layer, are shown in Figure S21 (PTQ10:Y6) and S21b (PM6:Y6). For devices using both BHJs (PM6:Y6 and PTQ10:Y6) the average V_{oc} remains almost the same with and without the PDIN-H layer on ZnO. However, with PDIN-H, the average PCE is increased in both cases due to the increase in average J_{sc} and FF, which is evident from the statistical plot. The average PCE follows the trend of average J_{sc} and FF.

The increase in PCE is due to an increase in both the short circuit current (J_{sc}) and the fill factor (FF) for both the BHJ systems. This result is attributed to the PDIN-H passivation of ZnO, where the PDIN-H creates a uniform, smooth organic hydrophobic surface with reduced/suppressed surface defects, commonly found in ZnO, therefore improving the J_{sc} and FF. This is confirmed with the average series and shunt resistances in the OPV devices. The average series resistance of the PTQ10:Y6 (spin coated at 2500 rpm) based OPV devices decreased from 96.2 Ω to 72.9 Ω and the average shunt resistance increased from 2038.4 Ω to 2185.4 Ω when PDIN-H is employed. The average series resistance of the PM6:Y6 (spin coated at 3000 rpm) based OPV devices decreased from 44.9 Ω to 42.8 Ω while the average shunt resistance increased from 1877.6 Ω to 2518.3 Ω when PDIN-H is employed.

Modification of the ZnO surface energy with π-conjugated materials has been shown to facilitate acceptor migration/separation to the ETL. This process is driven by similarities in these materials' hydrophobic surface energies (Figure S19), leading to improved electron extraction. This finding is supported by the work of Liu *et al.* where SAMs that were employed atop ZnO led to surface energy modifications that resulted in current enhancements and improved performance.[14] A recent report from Sadeghianlemraski *et al.* investigated PDIN-H as an ETL material atop of ZnO deposited from *n*-propanol with the use of NaOH.[16] PDIN-H was found to lower the work function of ZnO (4.5 eV) to 3.9 eV, while also improving the photostability of the OPV device.[16] Experiments under 780 hours of ultraviolet (UV) light (365 nm) irradiation were performed to induce recombination at the ETL. It was elucidated that PDIN-H demonstrated significant retention of photovoltaic parameters, which may be attributed to an improved ability of PDIN-H to block holes under UV irradiation. This in turn lowered surface recombination commonly occurring between the BHJ and ZnO ETL interface.[16] The reduced work function of the ZnO/PDIN-H hybrid ETL within the OPV device is beneficial for overall performance, as it closely matches the LUMO energy of Y6 (4.1 eV).[32] The energy level matching vastly improves the ohmic contact within the BHJ increasing the electron transfer (J_{sc} , Figure 6a) while retaining hole blocking for efficient energy conversion. To confirm the increase in J_{sc}, we conducted external quantum efficiency (EQE) measurements of the PM6:Y6 OPV devices, shown in Figure S22. We observe that the presence of PDIN-H does not alter photocurrent generation (ca. from 300 – 950 nm). However, the maximum EQE reached 70.1% for ZnO only based devices and 74.5% for ZnO/PDIN-H based devices, at 610 nm wavelength. Overall, the photocurrent generated with ZnO/PDIN-H based device is higher than the ZnO based device. The calculated J_{sc} from the EQE measurements were 20.0 mA/cm^2 and 21.9 mA/cm^2 for ZnO and ZnO/PDIN-H based devices,

respectively, which is coherent with the J-V measurements. The V_{oc} in each device remains almost the same irrespective of the PDIN-H presence.

Conclusion

In conclusion, we have modified an N-annulated PDI molecule with a Boc protecting group, which allowed green organic solvent solubility and solution processability *via* both spin-coating and slot-die coating. Thermal deprotection of PDIN-Boc at temperatures above 120 °C was demonstrated atop glass/ITO/ZnO and PET substrates to yield smooth and uniform PDIN-H films that were shown to be solvent resistant to common OPV fabrication solvents. PDIN-H films were then applied to inverted architecture OPVs comprised of PTQ10:Y6 and PM6:Y6 BHJ photoactive layers. Increases in J_{sc} and FF were observed in OPV systems fabricated and tested in ambient conditions. Overall, the PDIN-Boc allows for green solvent processability via roll-to-roll compatible processes, thermal conversion provides a robust solvent resistant electron transport layer film that promotes improved performance within inverted OPV devices.

Section 3.0 – Materials and Methods

OPV Device Fabrication: OPV devices were fabricated with inverted structures: ITO | ZnO | BHJ | MoOx | Ag and ITO | ZnO | PDIN-H | BHJ | MoOx | Ag. All the solution processing was conducted in an ambient environment. Pre-patterned ITO coated glass was cleaned ultrasonically with water, acetone, and IPA for 10 minutes each. Substrates were then treated with UV-ozone for 30 minutes. ZnO solution was prepared by dissolving zinc oxide acetate dihydrate (1.5 g) in 15 ml 2-methoxyethanol and 420 ml ethanolamine. The solution was kept at room temperature with stirring overnight. The resulting solution was spin coated on cleaned ITO glass at 4000 rpm for 40 seconds and thermally annealed at 200 °C for 20 minutes, in air.

PDIN-Boc deposition: PDIN-Boc (5 mg/ml) was dissolved in 2-methylanisole and stirred for 5 minutes. The resulting solution was spin coated on ZnO coated ITO/glass substrates at 4000 rpm for 40 seconds and thermally annealed at 200 °C for 20 minutes to convert PDIN-Boc to PDIN-H.

PTQ10:Y6 solution: PTQ10 (14.6 mg/ml) and Y6 (17.4 mg/ml) were dissolved in chloroform (CF) separately and stirred overnight. The PTQ10 and Y6 solutions were mixed in 1:1 ratio to achieve total concentration of 16 mg/ml with donor:acceptor ratio of 1:1.2. Before spin coating, 0.25% 1,8-diiodooctane (DIO) was added to the solution. The solution was then spin coated at 2000, 2500, or 3000 rpm. The resulting thin films were annealed at 100 °C for 10 minutes to drive off solvent.

PM6:Y6 solution: PM6 (14.6 mg/ml) and Y6 (17.4 mg/ml) were dissolved in chloroform (CF) separately and stirred overnight. The PM6 and Y6 solutions were mixed in 1:1 ratio to achieve total concentration of 16 mg/ml with donor:acceptor ratio of 1:1.2. Before spin coating, 0.5% Chloronaphthalene (CN) was added to the solution. The solution was then spin coated at 2000,

2500, or 3000 rpm. The resulting thin films were annealed at 100 °C for 10 minutes to drive off solvent.

The hole transport layer and top contact, MoOx (10 nm) and Ag (100 nm), were thermally evaporated. The active area of the OPV devices was 0.14 cm^2.

OPV Device Testing: The devices were tested in ambient environment with Keithley 2420 source measure unit and Newport solar simulator (Model: 92251A-1000) with an irradiation intensity of 100 mW/cm^2. External quantum efficiency (EQE) was measured in an ambient environment with a QEX7 Solar Cell Spectral Response/QE/IPCE Measurement System (PV Measurement, model QEX7, USA) with an optical lens to focus the light into an area about 0.04 cm^2, smaller than the cell. The silicon reference cell was used to calibrate the EQE measurement system in the wavelength range from 300 to 1100 nm.

General Procedure for Film Formation on Glass: Glass slides were cleaned with soap and water, acetone and isopropanol, and followed by UV/ozone treatment using a Novascan UV/ozone cleaning system. 45 uL of the ZnO solution (*vide supra*) was cast atop the glass and spun at 4000 rpm for 60 seconds. The films were then annealed at 200 ºC for 20 minutes, in air. 50 uL of the PDIN-Boc solution (1, 5, or 10 mg/mL) was then spin-cast atop the glass at 4000 rpm for 60 seconds. Films were thermally annealed at 200 ºC for 20 minutes to yield PDIN-H films.

Supporting information

Experimental details on materials synthesis and characterization: ^1H NMR, ^{13}C NMR, Mass spectrometry, Cyclic voltammetry, Differential pulse Voltammetry, Infrared Spectroscopy, Solvent resistance testing, Thermal annealing experiments, Large area deposition *via* slot-die coating, AMF imaging, Contact angle measurements, and GIWAXS measurements.

Acknowledgements

GCW acknowledges the CFI JELF (34102) and the University of Calgary. This research was undertaken thanks in part to funding from the Canada First Research Excellence Fund (CFREF). A portion of this work is supported by the National Science Foundation under grant award DMR-1608289. MAA was supported by the National Science Foundation under grant award DGE-1735173. Use of the Stanford Synchrotron Radiation Lightsource, SLAC National Accelerator Laboratory, is supported by the U.S. Department of Energy, Office of Science, Office of Basic Energy Sciences under Contract No. DE-AC02-76SF00515.

References

(1) Yin, Z.; Wei, J.; Zheng, Q. Interfacial Materials for Organic Solar Cells: Recent Advances and Perspectives. *Adv. Sci.* **2016**, *3* (8), 1500362. https://doi.org/10.1002/advs.201500362.

(2) Tian, L.; Xue, Q.; Hu, Z.; Huang, F. Recent Advances of Interface Engineering for Non-Fullerene Organic Solar Cells. *Org. Electron.* **2021**, *93* (February), 106141. https://doi.org/10.1016/j.orgel.2021.106141.

(3) Kyaw, A. K. K.; Sun, X. W.; Jiang, C. Y.; Lo, G. Q.; Zhao, D. W.; Kwong, D. L. An Inverted Organic Solar Cell Employing a Sol-Gel Derived ZnO Electron Selective Layer and Thermal Evaporated MoO3 Hole Selective Layer. *Appl. Phys. Lett.* **2008**, *93* (22), 221107. https://doi.org/10.1063/1.3039076.

(4) Sun, Y.; Seo, J. H.; Takacs, C. J.; Seifter, J.; Heeger, A. J. Inverted Polymer Solar Cells Integrated with a Low-Temperature-Annealed Sol-Gel-Derived ZnO Film as an Electron Transport Layer. *Adv. Mater.* **2011**, *23* (14), 1679–1683. https://doi.org/10.1002/adma.201004301.

(5) Zhang, X.; Yang, S.; Bi, S.; Kumaresan, A.; Zhou, J.; Seifter, J.; Mi, H.; Xu, Y.; Zhang, Y.; Zhou, H. Improved Electron Extraction by a ZnO Nanoparticle Interlayer for Solution-Processed Polymer Solar Cells. *RSC Adv.* **2017**, *7* (20), 12400–12406. https://doi.org/10.1039/C6RA28246F.

(6) Hau, S. K.; Yip, H.-L.; Baek, N. S.; Zou, J.; O'Malley, K.; Jen, A. K. Y. Air-Stable Inverted Flexible Polymer Solar Cells Using Zinc Oxide Nanoparticles as an Electron Selective Layer. *Appl. Phys. Lett.* **2008**, *92* (25), 253301. https://doi.org/10.1063/1.2945281.

(7) Tan, M. J.; Zhong, S.; Li, J.; Chen, Z.; Chen, W. Air-Stable Efficient Inverted Polymer Solar Cells Using Solution-Processed Nanocrystalline ZnO Interfacial Layer. *ACS Appl. Mater. Interfaces* **2013**, *5* (11), 4696–4701. https://doi.org/10.1021/am303004r.

(8) Prosa, M.; Tessarolo, M.; Bolognesi, M.; Margeat, O.; Gedefaw, D.; Gaceur, M.; Videlot-Ackermann, C.; Andersson, M. R.; Muccini, M.; Seri, M.; Ackermann, J. Enhanced Ultraviolet Stability of Air-Processed Polymer Solar Cells by Al Doping of the ZnO Interlayer. *ACS Appl. Mater. Interfaces* **2016**, *8* (3), 1635–1643. https://doi.org/10.1021/acsami.5b08255.

(9) Cowan, S. R.; Schulz, P.; Giordano, A. J.; Garcia, A.; MacLeod, B. A.; Marder, S. R.; Kahn, A.; Ginley, D. S.; Ratcliff, E. L.; Olson, D. C. Chemically Controlled Reversible and Irreversible Extraction Barriers Via Stable Interface Modification of Zinc Oxide Electron Collection Layer in Polycarbazole-Based Organic Solar Cells. *Adv. Funct. Mater.* **2014**, *24* (29), 4671–4680. https://doi.org/10.1002/adfm.201400158.

(10) Trost, S.; Behrendt, A.; Becker, T.; Polywka, A.; Görrn, P.; Riedl, T. Tin Oxide (SnO x) as Universal "Light-Soaking" Free Electron Extraction Material for Organic Solar Cells. *Adv. Energy Mater.* **2015**, *5* (17), 1500277. https://doi.org/10.1002/aenm.201500277.

(11) Trost, S.; Zilberberg, K.; Behrendt, A.; Polywka, A.; Görrn, P.; Reckers, P.; Maibach, J.; Mayer, T.; Riedl, T. Overcoming the "Light-Soaking" Issue in Inverted Organic Solar Cells by the Use of Al:ZnO Electron Extraction Layers. *Adv. Energy Mater.* **2013**, *3* (11), 1437–1444. https://doi.org/10.1002/aenm.201300402.

(12) Yao, J.; Qiu, B.; Zhang, Z.-G.; Xue, L.; Wang, R.; Zhang, C.; Chen, S.; Zhou, Q.; Sun, C.; Yang, C.; Xiao, M.; Meng, L.; Li, Y. Cathode Engineering with Perylene-Diimide Interlayer Enabling over 17% Efficiency Single-Junction Organic Solar Cells. *Nat. Commun.* **2020**, *11* (1), 2726. https://doi.org/10.1038/s41467-020-16509-w.

(13) Lange, I.; Reiter, S.; Pätzel, M.; Zykov, A.; Nefedov, A.; Hildebrandt, J.; Hecht, S.; Kowarik, S.; Wöll, C.; Heimel, G.; Neher, G. Tuning the Work Function of Polar Zinc Oxide Surfaces Using Modified Phosphonic Acid Self-Assembled Monolayers. *Adv. Funct. Mater.* **2014**, *24* (44), 7014–7024. https://doi.org/10.1002/adfm.201401493.

(14) Liu, H.; Liu, Z.; Wang, S.; Huang, J.; Ju, H.; Chen, Q.; Yu, J.; Chen, H.; Li, C. Boosting Organic–Metal Oxide Heterojunction via Conjugated Small Molecules for Efficient and Stable Nonfullerene Polymer Solar Cells. *Adv. Energy Mater.* **2019**, *9* (34), 1900887. https://doi.org/10.1002/aenm.201900887.

(15) Cornil, D.; Van Regemorter, T.; Beljonne, D.; Cornil, J. Work Function Shifts of a Zinc Oxide Surface upon Deposition of Self-Assembled Monolayers: A Theoretical Insight. *Phys. Chem. Chem. Phys.* **2014**, *16* (38), 20887–20899. https://doi.org/10.1039/C4CP02811B.

(16) Sadeghianlemraski, M.; Harding, C. R.; Welch, G. C.; Aziz, H. Significant Photostability Enhancement of Inverted Organic Solar Cells by Inserting an N-Annulated Perylene Diimide (PDIN-H) between the ZnO Electron Extraction Layer and the Organic Active Layer. *ACS Appl. Energy Mater.* **2020**, *3* (12), 11655–11665. https://doi.org/10.1021/acsaem.0c01587.

(17) Abd-Ellah, M.; Cann, J.; Dayneko, S. V.; Laventure, A.; Cieplechowicz, E.; Welch, G. C. Interfacial ZnO Modification Using a Carboxylic Acid Functionalized N-Annulated Perylene Diimide for Inverted Type Organic Photovoltaics. *ACS Appl. Electron. Mater.* **2019**, *1* (8), 1590–1596. https://doi.org/10.1021/acsaelm.9b00328.

(18) Yu, J.; Xi, Y.; Chueh, C.-C.; Zhao, D.; Lin, F.; Pozzo, L. D.; Tang, W.; Jen, A. K. Y. A Room-Temperature Processable PDI-Based Electron-Transporting Layer for Enhanced Performance in PDI-Based Non-Fullerene Solar Cells. *Adv. Mater. Interfaces* **2016**, *3* (18), 1600476. https://doi.org/10.1002/admi.201600476.

(19) Nian, L.; Zhang, W.; Wu, S.; Qin, L.; Liu, L.; Xie, Z.; Wu, H.; Ma, Y. Perylene Bisimide as a Promising Zinc Oxide Surface Modifier: Enhanced Interfacial Combination for Highly Efficient Inverted Polymer Solar Cells. *ACS Appl. Mater. Interfaces* **2015**, *7* (46), 25821–25827. https://doi.org/10.1021/acsami.5b07759.

(20) Wen, X.; Nowak-Król, A.; Nagler, O.; Kraus, F.; Zhu, N.; Zheng, N.; Müller, M.; Schmidt, D.; Xie, Z.; Würthner, F. Tetrahydroxy-Perylene Bisimide Embedded in a Zinc Oxide Thin Film as an Electron-Transporting Layer for High-Performance Non-Fullerene Organic Solar Cells. *Angew. Chemie Int. Ed.* **2019**, *58* (37), 13051–13055. https://doi.org/10.1002/anie.201907467.

(21) Harding, C. R.; Cann, J.; Laventure, A.; Sadeghianlemraski, M.; Abd-Ellah, M.; Rao, K. R.; Gelfand, B. S.; Aziz, H.; Kaake, L.; Risko, C.; Welch, G. C. Acid Dyeing for Green Solvent Processing of Solvent Resistant Semiconducting Organic Thin Films. *Mater. Horizons* **2020**, *7* (11), 2959–2969. https://doi.org/10.1039/D0MH00785D.

(22) Shaker, M.; Park, B.; Lee, J.-H.; Kim, W.; Trinh, C. K.; Lee, H.-J.; Choi, J. woo; Kim, H.; Lee, K.; Lee, J. Synthesis and Organic Field Effect Transistor Properties of Isoindigo/DPP-Based Polymers Containing a Thermolabile Group. *RSC Adv.* **2017**, *7* (27), 16302–16310. https://doi.org/10.1039/C7RA01726J.

(23) Guo, C.; Quinn, J.; Sun, B.; Li, Y. An Indigo-Based Polymer Bearing Thermocleavable Side Chains for n-Type Organic Thin Film Transistors. *J. Mater. Chem. C* **2015**, *3* (20), 5226–5232. https://doi.org/10.1039/C5TC00512D.

(24) Liu, C.; Dong, S.; Cai, P.; Liu, P.; Liu, S.; Chen, J.; Liu, F.; Ying, L.; Russell, T. P.; Huang, F.; Cao, Y. Donor–Acceptor Copolymers Based on Thermally Cleavable Indigo, Isoindigo, and DPP

Units: Synthesis, Field Effect Transistors, and Polymer Solar Cells. *ACS Appl. Mater. Interfaces* **2015**, *7* (17), 9038–9051. https://doi.org/10.1021/am5089956.

(25) Hendsbee, A. D.; Sun, J.-P. P.; Law, W. K.; Yan, H.; Hill, I. G.; Spasyuk, D. M.; Welch, G. C. Synthesis, Self-Assembly, and Solar Cell Performance of N-Annulated Perylene Diimide Non-Fullerene Acceptors. *Chem. Mater.* **2016**, *28* (19), 7098–7109. https://doi.org/10.1021/acs.chemmater.6b03292.

(26) Vespa, M.; Cann, J. R.; Dayneko, S. V.; Melville, O. A.; Hendsbee, A. D.; Zou, Y.; Lessard, B. H.; Welch, G. C. Synthesis of a Perylene Diimide Dimer with Pyrrolic N-H Bonds and N-Functionalized Derivatives for Organic Field-Effect Transistors and Organic Solar Cells. *European J. Org. Chem.* **2018**, *2018* (33), 4592–4599. https://doi.org/10.1002/ejoc.201801055.

(27) Ma, Z.; Zhao, B.; Gong, Y.; Deng, J.; Tan, Z. Green-Solvent-Processable Strategies for Achieving Large-Scale Manufacture of Organic Photovoltaics. *J. Mater. Chem. A* **2019**, *7* (40), 22826–22847. https://doi.org/10.1039/C9TA09277C.

(28) Zhang, K.; Chen, Z.; Armin, A.; Dong, S.; Xia, R.; Yip, H.-L.; Shoaee, S.; Huang, F.; Cao, Y. Efficient Large Area Organic Solar Cells Processed by Blade-Coating With Single-Component Green Solvent. *Sol. RRL* **2018**, *2* (1), 1700169. https://doi.org/10.1002/solr.201700169.

(29) Lee, J.; Kim, J. W.; Park, S. A.; Son, S. Y.; Choi, K.; Lee, W.; Kim, M.; Kim, J. Y.; Park, T. Study of Burn-In Loss in Green Solvent-Processed Ternary Blended Organic Photovoltaics Derived from UV-Crosslinkable Semiconducting Polymers and Nonfullerene Acceptors. *Adv. Energy Mater.* **2019**, *9* (34), 1901829. https://doi.org/10.1002/aenm.201901829.

(30) de Gennes, P. G. Wetting: Statics and Dynamics. *Rev. Mod. Phys.* **1985**, *57* (3), 827–863. https://doi.org/10.1103/RevModPhys.57.827.

(31) Faure, M. D. M.; Lessard, B. H. Layer-by-Layer Fabrication of Organic Photovoltaic Devices: Material Selection and Processing Conditions. *J. Mater. Chem. C* **2021**, *9* (1), 14–40. https://doi.org/10.1039/D0TC04146G.

(32) Yuan, J.; Zhang, Y.; Zhou, L.; Zhang, G.; Yip, H.-L.; Lau, T.-K.; Lu, X.; Zhu, C.; Peng, H.; Johnson, P. A.; Leclerc, M.; Cao, Y.; Ulanski, J.; Li, Y.; Zou, Y. Single-Junction Organic Solar Cell with over 15% Efficiency Using Fused-Ring Acceptor with Electron-Deficient Core. *Joule* **2019**, *3* (4), 1140–1151. https://doi.org/10.1016/j.joule.2019.01.004.

(33) Wu, Y.; Zheng, Y.; Yang, H.; Sun, C.; Dong, Y.; Cui, C.; Yan, H.; Li, Y. Rationally Pairing Photoactive Materials for High-Performance Polymer Solar Cells with Efficiency of 16.53%. *Sci. China Chem.* **2020**, *63* (2), 265–271. https://doi.org/10.1007/s11426-019-9599-1.

(34) Cui, Y.; Yao, H.; Zhang, J.; Zhang, T.; Wang, Y.; Hong, L.; Xian, K.; Xu, B.; Zhang, S.; Peng, J.; Wei, Z.; Gao, F.; Hou, J. Over 16% Efficiency Organic Photovoltaic Cells Enabled by a Chlorinated Acceptor with Increased Open-Circuit Voltages. *Nat. Commun.* **2019**, *10* (1), 2515. https://doi.org/10.1038/s41467-019-10351-5.

(35) Sun, C.; Pan, F.; Bin, H.; Zhang, J.; Xue, L.; Qiu, B.; Wei, Z.; Zhang, Z.-G.; Li, Y. A Low Cost and High Performance Polymer Donor Material for Polymer Solar Cells. *Nat. Commun.* **2018**, *9* (1), 743. https://doi.org/10.1038/s41467-018-03207-x.

TOC

New Perylene Diimide Modified Interlayers for Improved Organic Solar Cells